Nonlinear Observer for 3D Rigid Body Motion Estimation Using Doppler Measurements

Sérgio Brás, Maziar Izadi, Carlos Silvestre, Amit Sanyal, and Paulo Oliveira

***Abstract*—This work presents a nonlinear observer that estimates the translational and rotational motion of a rigid body based on measurements of configuration (pose), angular velocity, and radial velocity as well as modeled forces and torques. The radial velocity measurements are provided by a single direction Doppler sensor. Using a conveniently defined Lyapunov function, a nonlinear observer on the Special Euclidean Group (SE(3)) is derived and almost globally stability is guaranteed. The resulting estimation error is almost globally exponentially convergent for sufficiently rich motion. Numerical simulation results are presented that illustrate the performance of the proposed solution.**

***Index Terms*—Doppler measurements, navigation, nonlinear dynamic systems, observers, time-varying systems.**

I. Introduction

The accuracy of the position and attitude estimation system is key for the operation of many modern vehicles. Due to its importance, this problem has been the focus of intense research, which resulted in more accurate and efficient algorithms. However, regardless of its rich background, there are still challenges and open problems, some of which are related to the geometry of the state space. In particular, topological obstructions to global asymptotic stabilization by continuous state feedback for systems evolving on non-contractible manifolds are discussed in [1]–[4].

Some pose estimation solutions address the attitude motion separately from the translational motion. A position filter based on single range measurements is proposed in [5]. In [6] and [7], attitude estimation methods are devised which integrate measurements of angles or directions with inertial data provided by rate gyros. Other approaches consider an integrated framework to address the two estimation problems, as for instance in [8]–[10]. Thus, when a suitable dynamic model is available, it can be used together with the rigid body kinematics to improve the position and attitude estimates, as in [11]–[13].

New challenges to observer design arise when full state measurements are not available. An interesting case is when the translational velocity is measured by a Doppler sensor. This sensor measures the frequency shift of a signal that occurs when the source and the receiver have different velocities, i.e., the Doppler effect, and is nowadays currently used in the operation of many underwater vehicles as well as spacecrafts.

This work addresses the estimation of the complete translational velocity assuming that pose, angular velocity, and radial component of the tranlational velocity are measured. To that end, a nonlinear observer for the full rigid body motion in SE(3) is designed under the framework of geometric mechanics. The solution presented is derived explicitly using the exponential coordinates representation of SE(3), which is almost global in its description of the motion. If the position vector of the rigid body is persistently exciting, almost global exponential stability of the observer is guaranteed for noise-free sensor measurements. The observer proposed in this work contrasts with the solution derived in [14] by the authors since it does not rely on full state measurements.

The remainder of this work is organized as follows. Section II describes the rigid body equations of motion formulated explicitly on SE(3) and introduces the state (configuration and velocity) estimation problem. In Section III, a nonlinear observer that estimates pose and velocities is proposed, and its convergence and stability properties are analyzed. In Section IV, simulation results validating the performance of the proposed observer are presented. Finally, concluding remarks are given in Section V.

II. Problem Formulation and Measurement Model

Consider a body-fixed coordinate frame with origin at the center of mass of a rigid body denoted by $\{B\}$ and an inertially fixed reference frame denoted by $\{I\}$. Let the rotation matrix from $\{B\}$ to $\{I\}$ be given by $\mathbf{R}$ and the coordinates of the origin of $\{B\}$ with respect to $\{I\}$ be denoted by $\mathbf{b}$. The set of rotation matrices, which contains $\mathbf{R}$, is denoted by $\mathrm{SO}(3) = \{\mathbf{R} \in \mathbb{R}^{3\times 3} : \mathbf{R}^T\mathbf{R} = \mathbf{I}_3, \det(\mathbf{R}) = 1\}$, where $\mathbf{I}_n$ denotes the $n \times n$ identity matrix. The rigid body kinematics are given by

$$\dot{\mathbf{R}} = \mathbf{R}(\boldsymbol{\omega})^\times, \quad \dot{\mathbf{b}} = \mathbf{R}\mathbf{v},$$

where the translational and angular velocities expressed in the body fixed frame $\{B\}$ are denoted by $\mathbf{v}$ and $\boldsymbol{\omega}$, respectively, and the skew-symmetric operator $(.)^\times : \mathbb{R}^3 \to \mathfrak{so}(3)$ satisfies

$$(\boldsymbol{\omega})^\times = \begin{bmatrix} 0 & -\omega_z & \omega_y \\ \omega_z & 0 & -\omega_x \\ -\omega_y & \omega_x & 0 \end{bmatrix}.$$

Manuscript received March 10, 2014; revised November 15, 2014 and August 17, 2015; accepted January 19, 2016. Date of publication February 8, 2016; date of current version October 25, 2016. This work was supported by the Fundação para a Ciência e a Tecnologia (FCT) through ISR under LARSyS FCT [UID/EEA/50009/2013] and through IDMEC, under LAETA FCT [UID/EMS/50022/2013] projects, by the University of Macau, Macao, China, under Project MYRG2015-00126-FST, by the Macao Science and Technology Development Fund under Grant FDCT/048/2014/A1, by the Ph.D. Student Scholarship SFRH/BD/47456/2008, from FCT, and by the NSF under Grant CMMI 1131643. Recommended by Associate Editor L. Menini.

S. Brás is with ISR/LARSyS, Instituto Superior Técnico, Universidade de Lisboa, 1679-004 Lisboa, Portugal (e-mail: sbras@isr.ist.utl.pt).

M. Izadi is with the Department of Aerospace Engineering, Texas A&M University, College Station, TX 77840 USA (e-mail: maziar@tamu.edu).

C. Silvestre is with the Department of Electrical and Computer Engineering, Faculty of Science and Technology, University of Macau, Macau, China, on leave from the Instituto Superior Técnico, Universidade de Lisboa, 1679-004 Lisboa, Portugal (e-mail: csilvestre@umac.mo).

A. Sanyal is with Department of Mechanical and Aerospace Engineering, Syracuse University, Syracuse, NY 13244 USA (e-mail: aksanyal@syr.edu).

P. Oliveira is with IDMEC/LAETA and ISR/LARSyS, Instituto Superior Técnico, Universidade de Lisboa, 1679-004 Lisboa, Portugal (e-mail: p.oliveira@dem.ist.utl.pt).

Color versions of one or more of the figures in this paper are available online at http://ieeexplore.ieee.org.

Digital Object Identifier 10.1109/TAC.2016.2526671

The linear space $\mathfrak{so}(3)$ is the Lie algebra associated with the Lie group SO(3) and corresponds to the set of 3×3 skew-symmetric matrices.

Let $\mathcal{G}$ be the rigid body configuration, such that

$$\mathcal{G} = \begin{bmatrix} \mathbf{R} & \mathbf{b} \\ \mathbf{0}_{1\times 3} & 1 \end{bmatrix} \in \mathrm{SE}(3),$$

where $\mathbf{0}_{m\times n}$ denotes an $m \times n$ matrix whose elements are zero and the Lie group SE(3) is characterized by

$$\mathrm{SE}(3) = \left\{ \mathcal{G} \in \mathbb{R}^{4\times 4}, \mathcal{G} = \begin{bmatrix} \mathbf{R} & \mathbf{b} \\ \mathbf{0}_{1\times 3} & 1 \end{bmatrix} : \mathbf{R} \in \mathrm{SO}(3), \mathbf{b} \in \mathbb{R}^3 \right\}.$$

Using this representation, the kinematic equations take the form

$$\dot{\mathcal{G}} = \mathcal{G}\boldsymbol{\xi}^\vee,$$

where $\boldsymbol{\xi} = [\boldsymbol{\omega}^T \ \mathbf{v}^T]^T$ is the vector of body velocities and the vector space isomorphism $(.)^\vee : \mathbb{R}^6 \to \mathfrak{se}(3)$ is given by

$$\boldsymbol{\xi}^\vee = \begin{bmatrix} (\boldsymbol{\omega})^\times & \mathbf{v} \\ \mathbf{0}_{1\times 3} & 0 \end{bmatrix} \in \mathfrak{se}(3).$$

This space is constructed in a six-dimensional linear space tangent to SE(3) at the identity vector. The rigid body dynamics is given by

$$\mathbf{J}\dot{\boldsymbol{\omega}} = (\mathbf{J}\boldsymbol{\omega})^\times \boldsymbol{\omega} + \boldsymbol{\tau} \quad (1)$$

$$m\dot{\mathbf{v}} = (m\mathbf{v})^\times \boldsymbol{\omega} + \boldsymbol{\phi}, \quad (2)$$

where m and $\mathbf{J}$ denote the rigid body scalar mass and inertia matrix, respectively, $\boldsymbol{\phi}$ denotes the external force applied to the rigid body and $\boldsymbol{\tau}$ the external torque, both expressed in the body-fixed coordinate frame. The dynamic (1) and (2) can be expressed in compact form as

$$\mathbb{I}\dot{\boldsymbol{\xi}} = \boldsymbol{\Xi}(\mathbb{I}, \boldsymbol{\omega})\boldsymbol{\xi} + \boldsymbol{\varphi},$$

where $\boldsymbol{\varphi} = [\boldsymbol{\tau}^T \ \boldsymbol{\phi}^T]^T$, and

$$\mathbb{I} = \begin{bmatrix} \mathbf{J} & \mathbf{0}_{3\times 3} \\ \mathbf{0}_{3\times 3} & m\mathbf{I}_3 \end{bmatrix}, \quad \boldsymbol{\Xi}(\mathbb{I}, \boldsymbol{\omega}) = \begin{bmatrix} (\mathbf{J}\boldsymbol{\omega})^\times & \mathbf{0}_{3\times 3} \\ \mathbf{0}_{3\times 3} & -m(\boldsymbol{\omega})^\times \end{bmatrix}.$$

In many practical situations only partial state information is available from the sensor data. A particularly relevant case is when the translational velocity information is given by a Doppler sensor. Such sensors can be found for instance in underwater autonomous vehicles and in spacecrafts. A velocity sensor based on the Doppler effect measures the frequency shift between the emitted signal (electromagnetic or acoustic) and the received signal. This difference is proportional to the difference of velocities between emitter and receiver and is given by

$$\Delta f = \frac{\frac{d}{dt}\left(\|\mathbf{b}_r - \mathbf{b}_s\|\right)}{c} f_0, \quad (3)$$

where f_0 denotes the emitted frequency, c is the propagation velocity of the signal, and $\mathbf{b}_r$ and $\mathbf{b}_s$ denote the positions of the receiver and of the source, respectively. Thus, the Doppler measurement does not provide full velocity information but rather only radial velocity information. Without loss of generality, consider $\mathbf{b}_s$ the center of the inertial reference frame $\{I\}$ and consider a receiver installed onboard the vehicle so that $\mathbf{b}_r = \mathbf{b}$. Then, (3) can be rewritten as

$$\Delta f = \alpha_D \frac{\mathbf{b}^T}{\|\mathbf{b}\|}\dot{\mathbf{b}} = \alpha_D \frac{\mathbf{b}^T}{\|\mathbf{b}\|}\mathbf{R}\mathbf{v},$$

where $\alpha_D = f_0/c$. Along with the scalar measurement, one also has information regarding its direction $\mathbf{b}(t)/\|\mathbf{b}(t)\|$. Without loss of generality, let the emitter and the receiver be located at the origin of $\{I\}$ and $\{B\}$, respectively. Then, projected translational velocity is given by

$$\mathbf{v}_D(t) = \mathbf{R}^T \frac{\mathbf{b}(t)}{\|\mathbf{b}(t)\|}\Delta_f \alpha_D = \mathbf{d}(t)\mathbf{d}^T(t)\mathbf{v}(t)$$

where $\mathbf{d}(t) = \mathbf{R}^T(\mathbf{b}(t)/\|\mathbf{b}(t)\|)$.

Finally, let us now introduce $\boldsymbol{\xi}_D$, which comprises the angular velocity and the projected translational velocity

$$\boldsymbol{\xi}_D = \begin{bmatrix} \boldsymbol{\omega} \\ \mathbf{v}_D \end{bmatrix} = \mathbf{D}(t)\boldsymbol{\xi}, \quad \mathbf{D}(t) = \begin{bmatrix} \mathbf{I}_3 & \mathbf{0}_{3\times 3} \\ \mathbf{0}_{3\times 3} & \mathbf{d}(t)\mathbf{d}^T(t) \end{bmatrix}. \quad (4)$$

Remark 1: Notice that $\mathbf{b}$ is not required to be the vehicle's centre of mass. However, if convenient, the previous introduced Doppler sensor model can be easily adapted such that $\mathbf{b}$ is the centre of mass and $\mathbf{v}$ its translational velocity even if the receiver is not in such position.

Our aim is to design a dynamic nonlinear observer to estimate the configuration (pose), the angular velocity and, in particular, the translational velocity of a rigid body. The observer is based on exact measurements of pose ($\mathbf{R}$ and $\mathbf{b}$), angular velocity ($\boldsymbol{\omega}$), and Doppler measurements (Δf), as well as modeled forces and torques ($\boldsymbol{\phi}$ and $\boldsymbol{\tau}$, respectively). From the Doppler measurements, only the radial component of the translational velocity can be obtained. Moreover, notice that, in the presence of sensor noise, the use of an observer has clear advantages over the raw measurements as the sensor information is fused with the rigid body dynamics and the sensor noise is filtered. The resulting estimates are less noisy and the errors due to sensor bias have smaller magnitude than those of the raw sensor data. Robustness to bounded measurement errors is obtained consequently. This is shown later through numerical simulation results.

III. Observer Design With Doppler Measurements

In this section, we propose an observer for the configuration and velocity. Let us denote the configuration estimates by

$$\hat{\mathcal{G}} = \begin{bmatrix} \hat{\mathbf{R}} & \hat{\mathbf{b}} \\ \mathbf{0}_{1\times 3} & 1 \end{bmatrix},$$

where $\hat{\mathbf{R}}$ and $\hat{\mathbf{b}}$ are the estimated attitude and position, respectively. The estimated velocity is denoted by

$$\hat{\boldsymbol{\xi}} = \begin{bmatrix} \hat{\boldsymbol{\omega}} \\ \hat{\mathbf{v}} \end{bmatrix},$$

where $\boldsymbol{\omega}$ and $\mathbf{v}$ are the angular and translation velocity estimates, respectively. The configuration and velocity estimation errors are defined as

$$\tilde{\mathcal{G}} = \hat{\mathcal{G}}^{-1}\mathcal{G} = \begin{bmatrix} \tilde{\mathbf{R}} & -\tilde{\mathbf{R}}^T\tilde{\mathbf{b}} \\ \mathbf{0}_{1\times 3} & 1 \end{bmatrix} \in \mathrm{SE}(3)$$

$$\tilde{\boldsymbol{\xi}} = \hat{\boldsymbol{\xi}} - \boldsymbol{\xi} = \begin{bmatrix} \tilde{\boldsymbol{\omega}} \\ \tilde{\mathbf{v}} \end{bmatrix} \in \mathbb{R}^6, \quad (5)$$

where $\tilde{\mathbf{R}} = \hat{\mathbf{R}}^T\mathbf{R}$, $\tilde{\mathbf{b}} = \hat{\mathbf{b}} - \mathbf{b}$, $\tilde{\boldsymbol{\omega}} = \hat{\boldsymbol{\omega}} - \boldsymbol{\omega}$, and $\tilde{\mathbf{v}} = \hat{\mathbf{v}} - \mathbf{v}$. The configuration error can be expressed in exponential coordinates using

$$\tilde{\boldsymbol{\eta}}^\vee = \mathrm{logm}(\tilde{\mathcal{G}}), \quad (6)$$

where $\mathrm{logm}(.) : \mathrm{SE}(3) \to \mathfrak{se}(3)$ denotes the logarithmic map on SE(3) [15, p. 256]. We express the exponential coordinates vector of the pose estimate error $\tilde{\boldsymbol{\eta}}$ as

$$\tilde{\boldsymbol{\eta}} = \begin{bmatrix} \tilde{\boldsymbol{\Theta}} \\ \tilde{\boldsymbol{\beta}} \end{bmatrix} \in \mathbb{R}^6 \simeq \mathfrak{se}(3),$$

where $\tilde{\boldsymbol{\Theta}} \in \mathbb{R}^3 \simeq \mathfrak{so}(3)$ is the exponential coordinate vector (principal rotation vector) for the attitude estimation error and $\tilde{\boldsymbol{\beta}} \in \mathbb{R}^3$ is the exponential coordinate vector for the position estimate error.

The time derivative of configuration error (5) is given by

$$\begin{aligned}\dot{\tilde{\mathcal{G}}} &= \frac{d}{dt}(\hat{\mathcal{G}}^{-1})\mathcal{G} + \hat{\mathcal{G}}^{-1}\dot{\mathcal{G}} \\ &= -\hat{\mathcal{G}}^{-1}\dot{\hat{\mathcal{G}}}\hat{\mathcal{G}}^{-1}\mathcal{G} + \hat{\mathcal{G}}^{-1}\dot{\mathcal{G}} \\ &= -\hat{\mathcal{G}}^{-1}\dot{\hat{\mathcal{G}}}\tilde{\mathcal{G}} + \hat{\mathcal{G}}^{-1}\mathcal{G}\boldsymbol{\xi}^\vee \\ &= \tilde{\mathcal{G}}(\boldsymbol{\xi}^\vee - \mathrm{Ad}_{\tilde{\mathcal{G}}^{-1}}\hat{\mathcal{G}}^{-1}\dot{\hat{\mathcal{G}}}),\end{aligned}$$

where the adjoint action of $\mathcal{G} \in \mathrm{SE}(3)$ on $\boldsymbol{\zeta} \in \mathfrak{se}(3)$ is given by $\mathrm{Ad}_{\mathcal{G}}(\boldsymbol{\zeta}^\vee) = \mathcal{G}(\boldsymbol{\zeta}^\vee)\mathcal{G}^{-1}$ and it satisfies

$$\mathrm{Ad}_{\mathcal{G}}(\boldsymbol{\zeta}^\vee) = \left(\begin{bmatrix}\mathbf{R} & \mathbf{0}_{3\times3} \\ (\mathbf{b})^\times\mathbf{R} & \mathbf{R}\end{bmatrix}\boldsymbol{\zeta}\right)^\vee.$$

The velocity error dynamics is given by

$$\begin{aligned}\mathbb{I}\dot{\tilde{\boldsymbol{\xi}}} &= \mathbb{I}\dot{\hat{\boldsymbol{\xi}}} - \mathbb{I}\dot{\boldsymbol{\xi}} \\ &= \mathbb{I}\dot{\hat{\boldsymbol{\xi}}} - \boldsymbol{\Xi}(\mathbb{I}, \boldsymbol{\omega})\boldsymbol{\xi} - \boldsymbol{\varphi}.\end{aligned}$$

The time derivative of the exponential representation of $\tilde{\mathcal{G}}$ is given by [15]

$$\dot{\tilde{\boldsymbol{\eta}}} = G(\tilde{\boldsymbol{\eta}})\left(\boldsymbol{\xi} - \left(\mathrm{Ad}_{\tilde{\mathcal{G}}^{-1}}\hat{\mathcal{G}}^{-1}\dot{\hat{\mathcal{G}}}\right)^\wedge\right), \tag{7}$$

where $(.)^\wedge$ is such that $((\mathbf{a})^\vee)^\wedge = \mathbf{a}, \mathbf{a} \in \mathbb{R}^6$ and

$$G(\tilde{\boldsymbol{\eta}}) = \begin{bmatrix}A(\tilde{\boldsymbol{\Theta}}) & \mathbf{0}_{3\times3} \\ T(\tilde{\boldsymbol{\Theta}}, \tilde{\boldsymbol{\beta}}) & A(\tilde{\boldsymbol{\Theta}})\end{bmatrix}, \text{ with} \tag{8}$$

$$\begin{aligned}A(\tilde{\boldsymbol{\Theta}}) &= \mathbf{I}_3 + \frac{1}{2}\tilde{\boldsymbol{\Theta}}^\times + \left(\frac{1}{\theta^2} - \frac{1+\cos\theta}{2\theta\sin\theta}\right)\left(\tilde{\boldsymbol{\Theta}}^\times\right)^2 \\ S(\tilde{\boldsymbol{\Theta}}) &= \mathbf{I}_3 + \frac{1-\cos\theta}{\theta^2}\tilde{\boldsymbol{\Theta}}^\times + \frac{\theta - \sin\theta}{\theta^3}\left(\tilde{\boldsymbol{\Theta}}^\times\right)^2, \text{ and} \\ T(\tilde{\boldsymbol{\Theta}}, \tilde{\boldsymbol{\beta}}) &= \frac{1}{2}\left(S(\tilde{\boldsymbol{\Theta}})\tilde{\boldsymbol{\beta}}\right)^\times A(\tilde{\boldsymbol{\Theta}}) \\ &\quad + \left(\frac{1}{\theta^2} - \frac{1+\cos\theta}{2\theta\sin\theta}\right)\left[\tilde{\boldsymbol{\Theta}}\tilde{\boldsymbol{\beta}}^T + (\tilde{\boldsymbol{\Theta}}^T\tilde{\boldsymbol{\beta}})A(\tilde{\boldsymbol{\Theta}})\right] \\ &\quad - \frac{(1+\cos\theta)(\theta - \sin\theta)}{2\theta\sin^2\theta}S(\tilde{\boldsymbol{\Theta}})\tilde{\boldsymbol{\beta}}\tilde{\boldsymbol{\Theta}}^T \\ &\quad + \left(\frac{(1+\cos\theta)(\theta+\sin\theta)}{2\theta^3\sin^2\theta} - \frac{2}{\theta^4}\right)\tilde{\boldsymbol{\Theta}}^T\tilde{\boldsymbol{\beta}}\tilde{\boldsymbol{\Theta}}\tilde{\boldsymbol{\Theta}}^T,\end{aligned} \tag{9}$$

where $\theta = \|\tilde{\boldsymbol{\Theta}}\|$. The exponential coordinate vector $\tilde{\boldsymbol{\Theta}}$ for the rotational motion is obtained by inverting the Rodrigues' formula

$$R(\tilde{\boldsymbol{\Theta}}) = \mathbf{I}_3 + \frac{\sin\theta}{\theta}\tilde{\boldsymbol{\Theta}}^\times + \frac{1-\cos\theta}{\theta^2}\left((\tilde{\boldsymbol{\Theta}})^\times\right)^2,$$

which is a well-known formula to express the rotation matrix in terms of the exponential coordinates on SO(3).

Next, we prove lemmas useful to establish the convergence and stability properties of the nonlinear observer proposed later in this section.

Lemma 1: The matrix $G(\tilde{\boldsymbol{\eta}})$, which shows up in the kinematics (7), (8) for the exponential coordinates on SE(3), satisfies the relationship $G(\tilde{\boldsymbol{\eta}})\tilde{\boldsymbol{\eta}} = \tilde{\boldsymbol{\eta}}$.

Proof: Beginning with the expression for $G(\tilde{\boldsymbol{\eta}})$ given by (8), we evaluate

$$G(\tilde{\boldsymbol{\eta}})\tilde{\boldsymbol{\eta}} = \begin{bmatrix}A(\tilde{\boldsymbol{\Theta}})\tilde{\boldsymbol{\Theta}} \\ T(\tilde{\boldsymbol{\Theta}}, \tilde{\boldsymbol{\beta}})\tilde{\boldsymbol{\Theta}} + A(\tilde{\boldsymbol{\Theta}})\tilde{\boldsymbol{\beta}}\end{bmatrix}.$$

From the expression for $A(\tilde{\boldsymbol{\Theta}})$, it is clear that

$$A(\tilde{\boldsymbol{\Theta}})\tilde{\boldsymbol{\Theta}} = \tilde{\boldsymbol{\Theta}}.$$

On evaluation of the other component, after some algebra, we obtain

$$T(\tilde{\boldsymbol{\Theta}}, \tilde{\boldsymbol{\beta}})\tilde{\boldsymbol{\Theta}} = \tilde{\boldsymbol{\beta}} - A(\tilde{\boldsymbol{\Theta}})\tilde{\boldsymbol{\beta}}.$$

Therefore, we get

$$T(\tilde{\boldsymbol{\Theta}}, \tilde{\boldsymbol{\beta}})\tilde{\boldsymbol{\Theta}} + A(\tilde{\boldsymbol{\Theta}})\tilde{\boldsymbol{\beta}} = \tilde{\boldsymbol{\beta}},$$

which gives the desired result. □

Remark 2: In [16, p. 39], an expansion for $G(\tilde{\boldsymbol{\eta}})$ is given in terms of matrix powers of

$$\mathrm{ad}_{\tilde{\boldsymbol{\eta}}} = \begin{bmatrix}(\tilde{\boldsymbol{\Theta}})^\times & \mathbf{0}_{3\times3} \\ (\tilde{\boldsymbol{\beta}})^\times & (\tilde{\boldsymbol{\Theta}})^\times\end{bmatrix},$$

from which the result in Lemma 1 can be concluded given that $\mathrm{ad}_{\tilde{\boldsymbol{\eta}}}\tilde{\boldsymbol{\eta}} = \mathbf{0}$.

Lemma 2: The matrix $G(\tilde{\boldsymbol{\eta}})$ satisfies the following equality:

$$\mathbf{K}^{-1}G^T(\tilde{\boldsymbol{\eta}})\mathbf{K} = G^T(\mathbf{K}\tilde{\boldsymbol{\eta}}), \tag{10}$$

where $\mathbf{K} = \begin{bmatrix}\mathbf{I}_3 & \mathbf{0}_{3\times3} \\ \mathbf{0}_{3\times3} & k_2\mathbf{I}_3\end{bmatrix}, k_2 > 0$.

Proof: The left-hand side of (10) fulfills

$$\begin{aligned}\mathbf{K}^{-1}G^T(\tilde{\boldsymbol{\eta}})\mathbf{K} &= \begin{bmatrix}\mathbf{I} & \mathbf{0}_{3\times3} \\ \mathbf{0}_{3\times3} & k_2^{-1}\mathbf{I}\end{bmatrix}\begin{bmatrix}A^T(\tilde{\boldsymbol{\Theta}}) & T^T(\tilde{\boldsymbol{\Theta}}, \tilde{\boldsymbol{\beta}}) \\ \mathbf{0}_{3\times3} & A^T(\tilde{\boldsymbol{\Theta}})\end{bmatrix} \\ &\quad \times \begin{bmatrix}\mathbf{I} & \mathbf{0}_{3\times3} \\ \mathbf{0}_{3\times3} & k_2\mathbf{I}\end{bmatrix} \\ &= \begin{bmatrix}A^T(\tilde{\boldsymbol{\Theta}}) & k_2T^T(\tilde{\boldsymbol{\Theta}}, \tilde{\boldsymbol{\beta}}) \\ \mathbf{0}_{3\times3} & A^T(\tilde{\boldsymbol{\Theta}})\end{bmatrix}.\end{aligned}$$

On the other hand

$$G^T(\mathbf{K}\tilde{\boldsymbol{\eta}}) = \begin{bmatrix}A^T(\tilde{\boldsymbol{\Theta}}) & T^T(\tilde{\boldsymbol{\Theta}}, k_2\tilde{\boldsymbol{\beta}}) \\ \mathbf{0}_{3\times3} & A^T(\tilde{\boldsymbol{\Theta}})\end{bmatrix}.$$

Notice that $\tilde{\boldsymbol{\beta}}$ multiply each term of $T(\tilde{\boldsymbol{\Theta}}, \tilde{\boldsymbol{\beta}})$ in (9). Thus, $T(\tilde{\boldsymbol{\Theta}}, \tilde{\boldsymbol{\beta}})$ is proportional to the norm of $\tilde{\boldsymbol{\beta}}$, and consequently we have $k_2T(\tilde{\boldsymbol{\Theta}}, \tilde{\boldsymbol{\beta}}) = T(\tilde{\boldsymbol{\Theta}}, k_2\tilde{\boldsymbol{\beta}})$. □

The following theorem establishes the stability and convergence of the proposed observer.

Theorem 1: Assume that the rigid body pose ($\mathbf{R}$ and $\mathbf{b}$), angular velocity ($\boldsymbol{\omega}$), and Doppler shift (Δf) are measured and that the external forces and torques ($\boldsymbol{\varphi}$ and $\boldsymbol{\tau}$, respectively) can be accurately modeled. Moreover, let the configuration and velocity observer be described by

$$\dot{\hat{\mathcal{G}}} = \hat{\mathcal{G}}\left(\mathrm{Ad}_{\tilde{\mathcal{G}}}(\hat{\boldsymbol{\xi}} + k_1\tilde{\boldsymbol{\eta}})^\vee\right) \tag{11}$$

$$\begin{aligned}\mathbb{I}\dot{\hat{\boldsymbol{\xi}}} &= \boldsymbol{\Xi}(\mathbb{I}, \boldsymbol{\omega})\hat{\boldsymbol{\xi}} + \boldsymbol{\varphi} + \frac{1}{k_3}G^T(\mathbf{K}\tilde{\boldsymbol{\eta}})\tilde{\boldsymbol{\eta}} \\ &\quad + \frac{k_4}{k_3}\left(\boldsymbol{\xi}_D - \mathbf{D}(t)\hat{\boldsymbol{\xi}}\right),\end{aligned} \tag{12}$$

where $\mathbf{K} = \begin{bmatrix} \mathbf{I}_3 & \mathbf{0}_{3\times3} \\ \mathbf{0}_{3\times3} & k_2\mathbf{I}_3 \end{bmatrix}$, and where $k_1, k_2, k_3, k_4 > 0$ are such that the initial conditions satisfy the inequality

$$\|\tilde{\boldsymbol{\Theta}}_0\|^2 + k_2\mu\|\tilde{\mathbf{b}}_0\|^2 + k_3\tilde{\boldsymbol{\xi}}_0^T\mathbf{K}\mathbb{I}\tilde{\boldsymbol{\xi}}_0 < \pi^2, \tag{13}$$

where $\boldsymbol{\Theta}_0 = \boldsymbol{\Theta}(t_0)$, $\mathbf{b}_0 = \mathbf{b}(t_0)$, $\boldsymbol{\xi}_0 = \boldsymbol{\xi}(t_0)$, and $\mu = \sqrt{1+\pi^2/2}$. Then, there exists $\bar{\theta} < \pi$ rad such that for all $t > t_0$, the attitude error satisfies $\|\tilde{\boldsymbol{\Theta}}(t)\| < \bar{\theta}$ and the estimation error $\mathbf{x}(t) = [\tilde{\boldsymbol{\eta}}^T\ \tilde{\boldsymbol{\xi}}^T]^T$ is almost globally asymptotically stable.

Proof: Topological limitations precludes global asymptotic stability of the origin [2]. In fact, if $\theta = \pi$ rad, the exponential coordinates of the configuration error $\tilde{\boldsymbol{\eta}}$ cannot be computed without ambiguity. This proof is divided in two parts: (i) using a judiciously selected Lyapunov function establish that (13) is a sufficient condition to ensure that for all $t > t_0$, $\theta(t) < \pi$ rad and thus, the critical points where $\tilde{\boldsymbol{\eta}}$ is not well defined are not part of the error system trajectories and (ii) show that all system trajectories converge to the origin. To that end, consider the Lyapunov function candidate

$$V = \frac{1}{2}\tilde{\boldsymbol{\eta}}^T\mathbf{K}\tilde{\boldsymbol{\eta}} + \frac{k_3}{2}\tilde{\boldsymbol{\xi}}^T\mathbf{K}\mathbb{I}\tilde{\boldsymbol{\xi}}.$$

Taking its time derivative, one obtains

$$\begin{aligned}
\dot{V} &= \tilde{\boldsymbol{\eta}}^T G(\tilde{\boldsymbol{\eta}})\left(\boldsymbol{\xi} - (\mathrm{Ad}_{\tilde{\mathcal{G}}^{-1}}\hat{\mathcal{G}}^{-1}\dot{\hat{\mathcal{G}}})^{\wedge}\right) \\
&\quad + k_3\tilde{\boldsymbol{\xi}}\mathbf{K}\left(\mathbb{I}\dot{\tilde{\boldsymbol{\xi}}} - \boldsymbol{\Xi}(\mathbb{I},\boldsymbol{\omega})\boldsymbol{\xi} - \boldsymbol{\varphi}\right) \\
&= \tilde{\boldsymbol{\eta}}^T G(\tilde{\boldsymbol{\eta}})\left(\boldsymbol{\xi} - \left(\mathrm{Ad}_{\tilde{\mathcal{G}}^{-1}}\hat{\mathcal{G}}^{-1}\hat{\mathcal{G}}\mathrm{Ad}_{\tilde{\mathcal{G}}}(\hat{\boldsymbol{\xi}} + k_1\tilde{\boldsymbol{\eta}})^{\vee}\right)^{\wedge}\right) \\
&\quad + k_3\tilde{\boldsymbol{\xi}}\mathbf{K}\left(\boldsymbol{\Xi}(\mathbb{I},\boldsymbol{\omega})\hat{\boldsymbol{\xi}} + \boldsymbol{\varphi} + \frac{1}{k_3}G^T(\mathbf{K}\tilde{\boldsymbol{\eta}})\tilde{\boldsymbol{\eta}}\right. \\
&\quad\quad \left. + \frac{k_4}{k_3}\left(\boldsymbol{\xi}_D - \mathbf{D}(t)\hat{\boldsymbol{\xi}}\right) - \boldsymbol{\Xi}(\mathbb{I},\boldsymbol{\omega})\boldsymbol{\xi} - \boldsymbol{\varphi}\right) \\
&= \tilde{\boldsymbol{\eta}}^T G(\tilde{\boldsymbol{\eta}})(-\tilde{\boldsymbol{\xi}} - k_1\tilde{\boldsymbol{\eta}}) \\
&\quad + k_3\tilde{\boldsymbol{\xi}}\mathbf{K}\left(\boldsymbol{\Xi}(\mathbb{I},\boldsymbol{\omega})\tilde{\boldsymbol{\xi}} + \frac{1}{k_3}G^T(\mathbf{K}\tilde{\boldsymbol{\eta}})\tilde{\boldsymbol{\eta}}\right. \\
&\quad\quad \left. + \frac{k_4}{k_3}\left(\boldsymbol{\xi}_D - \mathbf{D}(t)\hat{\boldsymbol{\xi}}\right)\right).
\end{aligned}$$

From (4), we have $\boldsymbol{\xi}_D = \mathbf{D}(t)\boldsymbol{\xi}$ and by noticing that $\boldsymbol{\Xi}(\mathbb{I},\boldsymbol{\omega})\tilde{\boldsymbol{\xi}}$ is perpendicular to $\tilde{\boldsymbol{\xi}}$, the time derivative of V is given by

$$\dot{V} = \tilde{\boldsymbol{\eta}}^T G(\tilde{\boldsymbol{\eta}})(-\tilde{\boldsymbol{\xi}} - k_1\tilde{\boldsymbol{\eta}}) + \tilde{\boldsymbol{\xi}}\mathbf{K}\left(G^T(\mathbf{K}\tilde{\boldsymbol{\eta}})\tilde{\boldsymbol{\eta}} + k_4\mathbf{D}(t)\tilde{\boldsymbol{\xi}}\right).$$

Finally, using the result in Lemma 1 and Lemma 2 to update the Lyapunov function derivative, one obtains

$$\dot{V} = -k_1\tilde{\boldsymbol{\eta}}^T\mathbf{K}\tilde{\boldsymbol{\eta}} - k_4\tilde{\boldsymbol{\xi}}^T\mathbf{K}\mathbf{D}(t)\tilde{\boldsymbol{\xi}},$$

which is negative semi-definite.

Notice that, the exponential coordinates of the configuration error are related to $\tilde{\mathbf{R}}$ and $\tilde{\mathbf{b}}$ by [15, p. 256]

$$\begin{aligned}
\tilde{\boldsymbol{\Theta}} &= \frac{\theta}{2\sin\theta}(\tilde{\mathbf{R}} - \tilde{\mathbf{R}}^T)^{\otimes}, \cos\theta = \frac{\mathrm{tr}(\tilde{\mathbf{R}}) - 1}{2}, |\theta| < \pi \text{ rad} \\
\tilde{\boldsymbol{\beta}} &= S^{-1}(\tilde{\boldsymbol{\Theta}})\tilde{\mathbf{b}},
\end{aligned}$$

where $(.)^{\otimes}$ is the inverse of the $(.)^{\times}$ map, $\mathrm{tr}(.)$ denotes the trace operator, $\mathrm{tr}(\tilde{\mathbf{R}}) \neq -1$, and

$$S^{-1}(\tilde{\boldsymbol{\Theta}}) = \mathbf{I}_3 - \frac{1}{2}(\tilde{\boldsymbol{\Theta}})^{\times} + \frac{2\sin\theta - \theta(1-\cos\theta)}{2\theta^2\sin\theta}\left((\tilde{\boldsymbol{\Theta}})^{\times}\right)^2.$$

From the relation between matrix norms [17], one concludes

$$\left\|S^{-1}(\tilde{\boldsymbol{\Theta}})\tilde{\mathbf{b}}\right\| \leq \left\|S^{-1}(\tilde{\boldsymbol{\Theta}})\right\|_2 \|\tilde{\mathbf{b}}\| \leq \left\|S^{-1}(\tilde{\boldsymbol{\Theta}})\right\|_F \|\tilde{\mathbf{b}}\|,$$

where $\|.\|_2$ and $\|.\|_F$ denote the Euclidean and Frobenius norms of matrices, respectively. Through some algebraic manipulations one obtains $\|S^{-1}(\tilde{\boldsymbol{\Theta}})\|_F \leq \mu$. Hence

$$\|\tilde{\boldsymbol{\eta}}\|^2 \leq \|\tilde{\boldsymbol{\Theta}}\|^2 + \mu^2\|\tilde{\mathbf{b}}\|^2. \tag{14}$$

Consider the level set described by

$$C_V = \left\{\mathbf{x} : V(\mathbf{x}(t), t) \leq \frac{\pi^2}{2}\right\}.$$

Then, using (14), one can infer that the condition (13) guarantees that $\mathbf{x}(t_0) \in C_V$. As C_V is a positive invariant set, one concludes that, for all $t \geq t_0$, $\mathbf{x}(t) \in C_V$, which in turn yields $\mathbf{x}(t) \in C_V \Rightarrow \|\tilde{\boldsymbol{\Theta}}(t)\| \leq \pi$ rad. Thus, we have concluded the first part of the proof by establishing that condition (13) guarantees that the configuration error $\tilde{\boldsymbol{\eta}}$ can be computed from the sensor measurements and current estimates using (5) and (6).

To show that all system trajectories converge to the origin notice that $\dot{V}$ is negative semi-definite. On the other hand, for bounded angular velocity, $\ddot{V}$ is finite. Then, according to Barbalat's Lemma [18], $\dot{V} \to 0$, from which one concludes that $\|\tilde{\boldsymbol{\eta}}\| \to 0$. Since the configuration coordinates are bounded, this result implies that $(d/dt)\|\tilde{\boldsymbol{\eta}}\| \to 0$. Thus, $\|\tilde{\boldsymbol{\xi}}\| \to 0$ and consequently $\|\mathbf{x}\| \to 0$. □

Remark 3: The exponential coordinate $\tilde{\boldsymbol{\Theta}}$ for SO(3) cannot be uniquely obtained when $\theta = \|\tilde{\boldsymbol{\Theta}}\| = \pi$ rad, since in this case $\tilde{\boldsymbol{\Theta}}$ and $-\tilde{\boldsymbol{\Theta}}$ correspond to the same rotation matrix according to Rodrigues' formula. In such circumstances, the matrix $G(\tilde{\boldsymbol{\eta}})$ also becomes singular.

In case of a rich enough trajectory, a stronger result is obtained. To that end, consider the following definition.

Definition 1 (Persistency of Excitation—see [19]): A vector $\mathbf{z}(.)$ is said to be persistently exciting (PE) if there exist $T > 0$, $u_1 \geq 0$, and $u_2 \geq 0$ such that

$$u_1\mathbf{I} \leq \int_t^{t+T} \mathbf{z}(\tau)\mathbf{z}^T(\tau)d\tau \leq u_2\mathbf{I}, \qquad \forall\, t \geq t_0.$$

This definition states that a trajectory is rich if its position wobbles around enough in all time intervals of duration T. In fact, if the position of the rigid body is PE, the following result can be established.

Theorem 2: Assume that the rigid body pose ($\mathbf{R}$ and $\mathbf{b}$), angular velocity ($\boldsymbol{\omega}$), and Doppler shift (Δf) are measured and that the external forces and torques ($\boldsymbol{\varphi}$ and $\boldsymbol{\tau}$, respectively) can be accurately modeled. Let (11) and (12) describe the configuration and velocities observer, and $k_1, k_2, k_3, k_4 > 0$ be such that (13) holds. Moreover, assume that the position of the rigid body expressed in $\{B\}$ is PE. Then, the estimation error $\mathbf{x}(t)$ converges exponentially fast to the origin.

Proof: Without loss of generality let $t_0 = 0$. Under condition (13), the configuration error $\tilde{\boldsymbol{\eta}}$ can be retrieved from the sensor measurements and the current estimates. The Lyapunov function V fulfills

$$\gamma_1\|\mathbf{x}(t)\|^2 \leq V(\mathbf{x}_D, t) \leq \gamma_2\|\mathbf{x}(t)\|^2, \tag{15}$$

where $\gamma_1 = \min\{1, k_2, mk_2k_3, k_3\underline{\sigma}_{\mathbf{J}}\}$, $\gamma_2 = \max\{1, k_2, mk_2k_3, \bar{\sigma}_{\mathbf{J}}k_3\}$, and $\bar{\sigma}_{\mathbf{J}}$ and $\underline{\sigma}_{\mathbf{J}}$ denote the maximum and minimum singular values of $\mathbf{J}$, respectively. According to the premises of the theorem, the position of the rigid body expressed in the body fixed frame $\{B\}$ is PE. Thus, by Definition 1, there exist $T \geq 0$ and $u > 0$ such that

$$\int_t^{t+T} \mathbf{D}(\tau)d\tau \geq u\mathbf{I}, \quad \forall\, t \geq 0.$$

Hence, the following inequality holds:

$$\int_{t}^{t+T} \dot{V}(\mathbf{x},\tau)d\tau \leq -\gamma_3 \|\mathbf{x}(t)\|^2, \quad \forall t \geq 0, \tag{16}$$

where $\gamma_3 = \min\{k_1, k_1k_2, uk_3, uk_2k_3\}$. Then, we have

$$V(t+T) = V(t) + \int_{t}^{t+T} \dot{V}(\mathbf{x},\tau)d\tau. \tag{17}$$

Using (15) and (16), we obtain

$$V(t+T) \leq V(t) - \gamma_3 \|\mathbf{x}(t)\|^2 \leq V(t)\left(1 - \frac{\gamma_3}{\gamma_2}\right).$$

Let $1 - (\gamma_3/\gamma_2) = \lambda$ and $t = NT + t_r$, where $N \in \mathbb{N}^0$ and $t_r \in [0, T)$. Notice that, $\lambda < 1$, since by definition γ_2 and γ_3 are positive real numbers. Moreover, $\lambda > 0$, as shown in the following. By definition, if $\|\mathbf{x}(0)\| \neq 0$, $V(t+T) > 0$ for a finite t. Thus, from (17), we have

$$0 < V(t) + \int_{t}^{t+T} \dot{V}(\mathbf{x},\tau)d\tau.$$

From (15) and (16), we have $0 < \gamma_2\|\mathbf{x}(t)\|^2 - \gamma_3\|\mathbf{x}(t)\|$, for all $0 < t < \infty$. Then, $\gamma_2 > \gamma_3$ and consequently $\lambda > 0$.

Since $V(t)$ is a time decreasing function, we have

$$\begin{aligned} V(t) &\leq V(NT) \leq V((N-1)T)\lambda \\ &\leq V((N-2)T)\lambda^2 \leq V(0)\lambda^N \\ &\leq V(0)\lambda^{t/T} \end{aligned}$$

and from (15), we get $\gamma_1\|\mathbf{x}(t)\|^2 \leq \gamma_2\|\mathbf{x}(0)\|^2\lambda^{t/T}$. After some algebraic manipulations, we finally obtain

$$\|\mathbf{x}(t)\| \leq \sqrt{\frac{\gamma_2}{\gamma_1}} e^{-(t/2T)\log(1/\lambda)} \|\mathbf{x}(0)\|.$$

□

IV. Simulations

In this section, simulation results that illustrate the robustness and convergence properties of the proposed solution are presented. The sensor suite onboard the rigid body provides configuration and Doppler measurements. Moreover, it is considered that forces and torques are accurately modeled. The rigid body performs a typical trajectory, illustrated in Fig. 1. The inertia of the rigid body is assumed as

$$\mathbf{J} = \begin{bmatrix} 1.1 & 0 & 0 \\ 0 & 1 & 0 \\ 0 & 0 & 0.9 \end{bmatrix} \text{ kg.m}^2,$$

and its mass is assumed as $m = 2$ kg. The simulation parameters are set to $k_1 = 1$, $k_2 = 1$, $k_3 = 1$, $k_4 = 4$, $\tilde{\boldsymbol{\Theta}}(t_0) = [-0.4 \;\; -0.2 \;\; -0.1]^T$ rad, $\tilde{\boldsymbol{\beta}} = [-1.073 \;\; -0.349 \;\; 0.488]^T$ m, $\tilde{\boldsymbol{\omega}}(t_0) = 10^{-3}[7\;4\;10]^T$ rad/s, and $\tilde{\mathbf{v}}(t_0) = 10^{-3}[10\;0\;-5]^T$ m/s. Note that, with these parameters, the condition (13) is satisfied.

Fig. 2 shows the time-evolution of the estimation error of the translational velocity, a quantity not measured by the sensors. As established in the previous section, the estimated translational velocity converges exponentially fast for its actual value.

The convergence and robustness properties of the estimation error of the proposed observer are illustrated in Fig. 3. In the lower plot, a logarithmic scale is adopted to highlight the exponentially fast convergence of the estimation error to the origin. Since the proposed observer is exponentially stable, the estimation error in presence

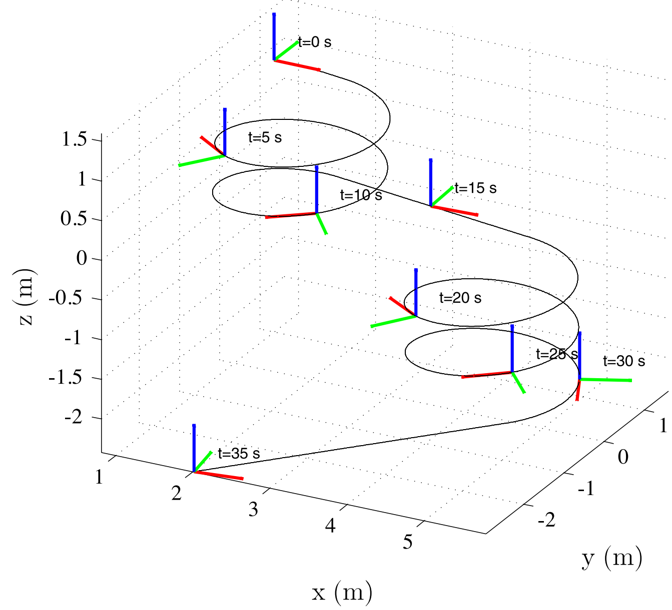

Fig. 1. Rigid body trajectory.

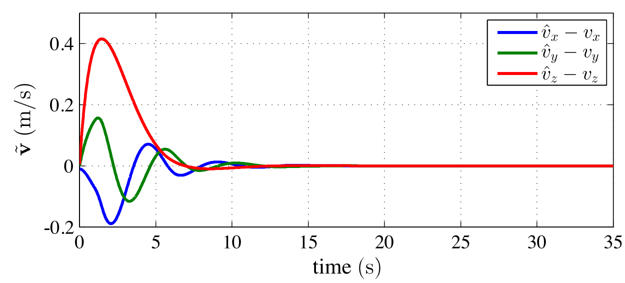

Fig. 2. Time-evolution of the translational velocity estimated with noise-free measurements.

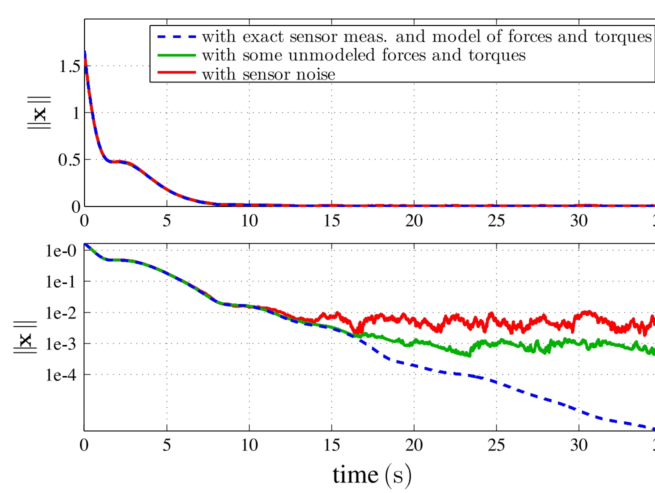

Fig. 3. Norm of the estimation error of the observer under perfect conditions, under unmodeled disturbances forces and torques and with the noise in all sensors.

of disturbances in the torques and forces is ultimately bounded [18, Theorem 4.16 and Theorem 4.18]. This robustness property is also illustrated in Fig. 3, where the estimation error is depicted for the case when there are unmodeled disturbances in the torques and forces, which are assumed to be random variables with uniform distribution and amplitude of 0.01 Nm and 0.1 N in each axis, respectively.

Additionally, Fig. 3 also depicts the results without disturbances but with noise in all sensor measurements to show the advantages of the estimated quantities when compared with the direct sensor measurements. The noise characteristics are given by $\mathrm{std}(\boldsymbol{\Theta}) = 0.01$ rad, $\mathrm{std}(\mathbf{b}) = 0.01$ m, $\mathrm{std}(\boldsymbol{\omega}) = 0.01$ rad/s and $\mathrm{std}(\mathbf{d}^T\mathbf{v}) = 0.01$ m/s, where std(.) denotes the standard deviation of each axis of the sensor. The standard deviation of the resulting estimates after the initial transient ($t > 15$ s) are

$$\mathrm{std}(\hat{\boldsymbol{\Theta}}) = \begin{bmatrix} 0.0009 \\ 0.0007 \\ 0.0006 \end{bmatrix} \text{ rad}, \qquad \mathrm{std}(\hat{\mathbf{b}}) = \begin{bmatrix} 0.0019 \\ 0.0026 \\ 0.0023 \end{bmatrix} \text{ m}$$

$$\mathrm{std}(\hat{\boldsymbol{\omega}}) = \begin{bmatrix} 0.0009 \\ 0.0010 \\ 0.0006 \end{bmatrix} \text{ rad/s}, \quad \mathrm{std}(\hat{\mathbf{v}}) = \begin{bmatrix} 0.0009 \\ 0.0011 \\ 0.0013 \end{bmatrix} \text{ m/s}.$$

Note the higher accuracy of the estimates when compared with the sensor measurements.

V. Conclusion

A nonlinear observer for arbitrary rigid body motion that takes advantage of Doppler data was obtained and expressed in terms of the exponential coordinates on the group of rigid body motions in the three-dimensional Euclidean space. The estimation error was shown to be asymptotically stable whenever the exponential coordinates are defined, which includes all attitude estimate errors except for those corresponding to a principal rotation angle of 180 deg or π rad. Therefore, the convergence of the estimates given by this observer was shown to be almost global over the state space of rigid body motions. Given persistency of excitation of the position vector of the rigid body, almost global exponential stability of the observer is guaranteed. Numerical simulation results confirmed the convergence and stability properties of the observer.

References

[1] D. Koditschek, "The application of total energy as a Lyapunov function for mechanical control systems," *Control Theory Multibody Syst.*, vol. 97, pp. 131–151, 1989.

[2] S. Bhat and D. Bernstein, "A topological obstruction to continuous global stabilization of rotational motion and the unwinding phenomenon," *Syst. Control Lett.*, vol. 39, no. 1, pp. 63–70, Jan. 2000.

[3] D. Fragopoulos and M. Innocenti, "Stability considerations in quaternion attitude control using discontinuous Lyapunov functions," *IEE Proc. Control Theory Appl.*, vol. 151, no. 3, pp. 253–258, May 2004.

[4] M. Malisoff, M. Krichman, and E. Sontag, "Global stabilization for systems evolving on manifolds," *J. Dynam. Control Syst.*, vol. 12, no. 2, pp. 161–184, Apr. 2006.

[5] P. Batista, C. Silvestre, and P. Oliveira, "Single range aided navigation and source localization: Observability and filter design," *Syst. Control Lett.*, vol. 60, no. 8, pp. 665–673, 2011.

[6] H. Rehbinder and X. Hu, "Drift-free attitude estimation for accelerated rigid bodies," *Automatica*, vol. 40, no. 4, pp. 653–659, 2004.

[7] M. Zamani, J. Trumpf, and R. Mahony, "Near-optimal deterministic filtering on the rotation group," *IEEE Trans. Autom. Control*, vol. 56, no. 6, pp. 1411–1414, Jun. 2011.

[8] J. Vasconcelos, R. Cunha, C. Silvestre, and P. Oliveira, "A nonlinear position and attitude observer on SE(3) using landmark measurements," *Syst. Control Lett.*, vol. 59, no. 3/4, pp. 155–166, 2010.

[9] C. Lageman, J. Trumpf, and R. Mahony, "Gradient-like observers for invariant dynamics on a Lie group," *IEEE Trans. Autom. Control*, vol. 55, no. 2, pp. 367–377, Feb. 2010.

[10] S. Rodrigues, N. Crasta, A. Aguiar, and F. Leite, "An exponential observer for systems on SE(3) with implicit outputs," in *Dynamics, Games and Science II*, ser. Springer Proceedings in Mathematics. Berlin/Heidelberg, Germany: Springer-Verlag, 2011, vol. 2, pp. 611–633.

[11] S. Salcudean, "A globally convergent angular velocity observer for rigid body motion," *IEEE Trans. Autom. Control*, vol. 36, no. 12, pp. 1493–1497, Dec. 1991.

[12] J. Vasconcelos, C. Silvestre, P. Oliveira, and B. Guerreiro, "Embedded UAV model and LASER aiding techniques for inertial navigation systems," *Control Eng. Prac.*, vol. 18, no. 3, pp. 262–278, 2010.

[13] A. Sanyal, T. Lee, M. Leok, and N. McClamroch, "Global optimal attitude estimation using uncertainty ellipsoids," *Syst. Control Lett.*, vol. 57, no. 3, pp. 236–245, 2008.

[14] S. Brás, M. Izadi, C. Silvestre, A. Sanyal, and P. Oliveira, "Nonlinear observer for 3D rigid body motion," in *Proc. 52nd IEEE Conf. Decision Control*, Florence, Italy, Dec. 2013.

[15] F. Bullo and A. Lewis, *Geometric Control of Mechanical Systems*, ser. Texts in Applied Mathematics. New York/Heidelberg/Berlin: Springer–Verlag, 2004, vol. 49.

[16] A. Bonfiglioli and R. Fulci, *Topics in Noncommutative Algebra: The Theorem of Campbell, Baker, Hausdorff and Dynkin*, ser. Lecture Notes in Mathematics. New York: Springer-Verlag, 2012.

[17] G. Golub and C. Van Loan, *Matrix Computations*, 3rd ed. Baltimore, MD, USA: The Johns Hopkins Univ. Press, 1996.

[18] H. Khalil, *Nonlinear Systems*, 3rd ed. Upper Saddle River, NJ, USA: Prentice-Hall, 2002.

[19] S. Sastry, *Nonlinear Systems: Analysis, Stability and Control*, ser. Interdisciplinary applied mathematics: Systems and control. New York, NY, USA: Springer-Verlag, 1999.